Published in final edited form as:
Biochem Pharmacol. 2011 April 1; 81(7): 934–941. doi:10.1016/j.bcp.2011.01.012.

PPARγ activation redirects macrophage cholesterol from fecal excretion to adipose tissue uptake in mice via SR-BI

Sue-Anne Toh[a,b,c,*], **John S. Millar**[b,c], **Jeffrey Billheimer**[b,d], **Ilia Fuki**[b], **Snehal U. Naik**[b], **Colin Macphee**[e], **Max Walker**[e], and **Daniel J. Rader**[b,c,d,**]

[a]Division of Endocrinology, Diabetes and Metabolism, University of Pennsylvania School of Medicine, Philadelphia, PA, USA

[b]Institute for Translational Medicine and Therapeutics, University of Pennsylvania School of Medicine, Philadelphia, PA, USA

[c]Institute of Diabetes, Obesity and Metabolism, University of Pennsylvania School of Medicine, Philadelphia, PA, USA

[d]Cardiovascular Institute, University of Pennsylvania School of Medicine, Philadelphia, PA, USA

[e]GlaxoSmithKline, King of Prussia, PA, USA

Abstract

PPARγ agonists, used in the treatment of Type 2 diabetes, can raise HDL-cholesterol, therefore could potentially stimulate macrophage-to-feces reverse cholesterol transport (RCT). We aimed to test whether PPARγ activation promotes macrophage RCT in vivo. Macrophage RCT was assessed in mice using cholesterol loaded/^{3}H-cholesterol labeled macrophages. PPARγ agonist GW7845 (20 mg/kg/day) did not change ^{3}H-tracer plasma appearance, but surprisingly decreased fecal ^{3}H-free sterol excretion by 43% ($P < 0.01$) over 48 h. Total free cholesterol efflux from macrophages to serum (collected from control and GW7845 groups) was not different, although ABCA1-mediated efflux was significantly higher with GW7845. To determine the effect of PPARγ activation on HDL cholesterol uptake by different tissues, the metabolic fate of HDL labeled with ^{3}H-cholesteryl ether (CE) was also measured. We observed two-fold increase in HDL derived ^{3}H-CE uptake by adipose tissue ($P < 0.005$) with concomitant 22% decrease in HDL derived ^{3}H-CE uptake by the liver ($P < 0.05$) in GW7845 treated wild type mice. This was associated with a significant increase in SR-BI protein expression in adipose tissue, but not liver. The same experiment in SR-BI knockout mice, showed no difference in HDL derived ^{3}H-CE uptake by adipose tissue or liver. In conclusion, PPARγ activation decreases the fecal excretion of macrophage derived cholesterol in mice. This is not due to inhibition of cholesterol efflux from macrophages, but rather involves redirection of effluxed cholesterol from liver towards adipose tissue uptake via SR-BI. This represents a novel mechanism for regulation of RCT and may extend the therapeutic implications of these ligands.

[*]Corresponding author at: Division of Endocrinology, Department of Medicine, National University of Singapore Health System, 1E Kent Ridge Road, NUHS Tower Block, Level 10, Singapore 119228, Singapore. Tel.: +65 6772 2195/90012612; fax: +65 68724101/67794112, s.e.s.toh.97@cantab.net, drstes8@yahoo.co.uk, sue_anne_toh@nuhs.edu.sg (S.-A. Toh). [**]Corresponding author at: University of Pennsylvania School of Medicine, 654 BRBII/III Labs, 421 Curie Blvd., Philadelphia, PA 19104, USA. Tel.: +1 215 573 4176; fax: +1 215 573 8606. rader@mail.med.upenn.edu (D.J. Rader).

Disclosure

Dr. Colin Macphee and Dr. Max Walker are full-time employees of GlaxoSmithKline. Dr. Rader has served as a consultant to and has received research funding from GlaxoSmithKline.

Appendix A. Supplementary data

Supplementary data associated with this article can be found, in the online version, at doi:10.1016/j.bcp.2011.01.012.

Keywords

PPARγ; HDL; Reverse cholesterol transport; Adipose tissue; SR-BI

1. Introduction

PPARγ is highly expressed in adipose tissue, where it is required for adipocyte differentiation [1,2], hence potentially contributing to obesity and its associated increased risks for insulin resistance and cardiovascular disease (CVD). PPARγ is also expressed in macrophages, where PPARγ-dependent lipid uptake and storage may increase foam-cell formation and, potentially, atherosclerosis [3]. Yet high affinity PPARγ agonists, the thiazolidinediones (TZDs), used in the treatment of Type 2 diabetes, are clinically effective at improving insulin sensitivity and lipid homeostasis [4,5], which would be expected to reduce CVD risk. Consistent with this, PPARγ ligands attenuate atherosclerosis in mice, albeit via uncertain mechanisms [6]. The effect of activation of PPARγ with TZDs on CVD outcomes in patients with Type 2 diabetes has been mixed, with some studies showing a possible increase in risk of myocardial infarction [7], and others showing a reduction in CVD risk [8]. Hence, the overall effect of PPARγ agonists on CVD and the mechanisms involved remain controversial and unclear.

The risk of CVD is inversely associated with plasma levels of high density lipoprotein cholesterol (HDL-C), and low HDL-C levels are often associated with insulin resistance [8]. The major atheroprotective mechanism of HDL is thought to involve facilitation of peripheral cholesterol efflux from lipid laden macrophages in the atherosclerotic plaque, and facilitation of its return to the liver for excretion in bile and feces [9], a process termed “reverse cholesterol transport” (RCT). The simplest paradigm for anti-atherosclerotic therapeutic development involving HDL-C would be one in which raising plasma concentrations of HDL-C or its major apolipoprotein apoA-I reliably translated into reduced atherosclerosis. However, it is plausible that certain approaches could improve HDL function without increasing plasma concentrations of HDL-C. For example, flux through the RCT pathway could be increased without increasing the steady-state level of HDL-C [10]. Another possibility is that one or more components in the RCT pathway are beneficial and the entire RCT pathway is not necessarily required for cardioprotective effects.

Both of the currently prescribed TZDs, rosiglitazone and pioglitazone, can raise HDL in patients with Type 2 diabetes [11], and PPARγ agonists have been suggested to be able to promote macrophage cholesterol efflux in vitro [12,13], but the effect of PPARγ agonists on RCT in vivo has not been systematically studied. The aim of this study was to investigate the effects of PPARγ activation on macrophage to feces RCT in vivo, as well as intermediate steps in the RCT pathway. Surprisingly, we found that in female wild-type C57BL6J mice, PPARγ agonist treatment decreased fecal sterol excretion in vivo, implying decreased RCT. This led us to hypothesize that PPARγ activation may be inhibiting macrophage cholesterol efflux (the first step in the RCT pathway), and/or redirecting effluxed cholesterol to other tissues. We systematically tested this hypothesis by performing macrophage cholesterol efflux studies in vitro and HDL cholesterol uptake studies in vivo with a potent and selective PPARγ agonist, GW7845.

2. Material and methods

2.1. Animals and diets

Wild-type C57BL/6 female mice (8–12 weeks-old) were obtained from the Jackson Laboratory (Bar Harbor, ME). SR-BI knockout mice were originally purchased from The

Jackson Laboratory and subsequently bred in-house. In all studies, the mice were matched for age, gender, and weight. Mice were fed ad libitum for 2 weeks with either a control or PPARγ agonist GW7845 (20 mg/kg/day), provided by GlaxoSmithKline (King of Prussia, PA), supplemented chow diet (Purina #5002; Research Diets Inc., New Brunswick, NJ). This dose and duration of treatment with GW7845 was selected based on efficacy demonstrated in pilot experiments. In our initial studies, we measured food intake and found this to be no different between control and GW7845 treated groups (22.2 g/mouse/week versus 22.1 g/mouse/week). Subsequently, we just measured body weights before and after 2 weeks of treatment to control for any potential effect(s) PPARγ agonist treatment may have on food intake and/or body weight. For plasma lipid analysis, animals were fasted for 4 h and then bled from the retro-orbital plexus. All animals were housed according to guidelines of the Institutional Animal Care and Use Committee of the University of Pennsylvania. All protocols were approved by the Institutional Animal Care and Use Committee.

2.2. Plasma lipid analysis

Plasma total cholesterol, HDL-cholesterol and triglycerides were measured on a Cobas Fara with the use of Sigma Diagnostic reagents (Sigma–Aldrich, St. Louis, MO).

2.3. Preparation of J774 cells for in vivo reverse cholesterol transport study

J774 cells, obtained from the American Type Culture Collection (ATCC; Manassas, VA), were grown in suspension in RPMI/HEPES supplemented with 10% FBS and 0.5% gentamicin. J774 cells were cultured in suspension in Nalgene Teflon flasks (Fisher Scientific, Hudson, NH) and radiolabeled with 5 μCi/mL ^{3}H-cholesterol and cholesterol loaded with 25 μg/mL acetylated LDL (acLDL), as previously described [14]. After forty-eight hours, radiolabeled cells were washed with RPMI/HEPES and equilibrated for 4 h in fresh RPMI/HEPES supplemented with 0.2% BSA and gentamicin. Cells were pelleted by low speed centrifugation and re-suspended in RPMI/HEPES prior to injection into mice.

2.4. In vivo reverse cholesterol transport study

[^{3}H]-Cholesterol-labeled and acLDL-loaded J774 cells (typically 4.5×10^{6} cells containing 4×10^{6} cpm of [^{3}H]-cholesterol in 0.5 mL minimum essential medium) were injected intraperitoneally into individually caged mice as described previously [14]. Mice had free access to food and water. Blood was collected at 6, 24, and 48 h to measure radioactivity released into plasma. Feces were collected continuously from 0 to 48 h and stored at 4 °C before extraction of cholesterol.

2.5. Preparation of bone marrow-derived macrophages

C57BL6/J mice were euthanized and dissected to remove the femur of each hind leg. Bone marrow was flushed from femur and tibia of each leg using PBS–heparin (100 μg/ml). Cells were washed with PBS and resuspended in bone marrow growth medium (DMEM containing 30% L-929 cell conditioned medium and 10% FBS). Bone marrow-derived cells were seeded in 12-well plates (for in vitro experiments) and cultured at 37 °C and 5% CO2. Four days after plating, nonadherent cells were removed by washing. Adherent cells were fed with fresh bone marrow growth medium and cultured for an additional 3 days. Aliquots of bone marrow-derived cells were analyzed for expression of markers specific for macrophages (CD11b, CD18), T-lymphocytes (TCRb) and B-lymphocytes CD19. After 7 days in culture under our experimental conditions, more than 99% of cells subcloned from bone marrow using L-929 conditioned medium (collected from plates) were positive for CD11b and CD18, while less that 1% of cells were positive for TCRβ or CD19, markers of T- or B-cells, respectively.

2.6. Measurement of cholesterol efflux in vitro, using plasma from PPARγ agonist treated mice

For in vitro efflux studies, BMMs were isolated and grown in 12-well plates as described above followed by labelling with ^{3}H-cholesterol (5 μCi/mL) (PerkinElmer Analytical Sciences, Boston, MA) in the presence of acLDL (25 μg/mL) for 24 h. Then cells were washed and equilibrated overnight in serum-free medium. For the cholesterol efflux, medium containing 2.5% mouse serum from either PPARγ agonist treated or control chow fed mice was added to cells. After 4 h, aliquots of the medium were removed, and the ^{3}H-cholesterol released into the medium was measured by liquid scintillation counting. The ^{3}H-cholesterol present in the cells was determined by extracting the cell lipids with isopropanol (Sigma–Aldrich, St. Louis, MO) and measured by liquid scintillation counting. To assess the relative contribution of ABCA1-dependent pathway, cells were pretreated with probucol (20 μM) (Sigma–Aldrich, St. Louis, MO), an ABCA1 inhibitor, for 2 h before measuring efflux of free cholesterol.

2.7. In vivo HDL cholesterol turn over studies

HDL was prepared from pooled human plasma by sequential ultracentrifugation (density $1.063 < d < 1.21$ g/mL). After extensive dialysis against dialysis buffer (0.15 M NaCl, EDTA 1 mM, pH 7.4), HDL was exchange labeled with ^{3}H-cholesteryl hexadecyl ether (cholesteryl-1,2-^{3}H; PerkinElmer Analytical Sciences, Boston, MA), as previously described [15]. After labelling, the HDL was reisolated by ultracentrifugation (density $1.063 < d < 1.21$ g/mL), extensively dialyzed, filter sterilized and stored at 4 °C until injection.

To measure the HDL fractional catabolic rate (FCR) and organ uptake of the HDL-cholesteryl esters, ^{3}H-cholesteryl ether-labeled HDL (approximately 1 million cpm per animal) was injected intravenously via tail veins into mice ($n = 6$ per group). Blood samples were drawn by retroorbital bleeding at 2 min, 1 h, 3 h, 6 h, 9 h, 24 h and 48 h (≈25 μL at each time point). At study termination (48 h after injection), mice were exsanguinated, perfused with ice cold PBS and liver and inguinal adipose tissue samples were collected for analysis. A portion of liver and adipose samples were placed in RNA later (Ambion) and stored at −80 °C for mRNA expression analysis.

Plasma decay curves for the tracer were normalized to radioactivity at the initial 2-min time point after tracer injection. FCRs were calculated from the area under the plasma disappearance curves fitted to a two compartment model, using WinSAAM modelling software. The HDL cholesteryl esters pool size, calculated by multiplying the HDL cholesteryl esters concentration by the plasma volume (3.5% of the body weight), was multiplied by the FCR to obtain the absolute production rate (APR). To measure the organ uptake of HDL-^{3}H-cholesteryl ether, lipid extraction was performed according to the procedure of Bligh and Dyer [16]. Briefly, a 50-mg piece of tissue was homogenized in water, and then lipids were extracted with a mixture of chloroform/methanol 2:1 (v/v). The lipid layer was collected, evaporated, resuspended in toluene, and counted in a liquid scintillation counter (LSC).

Organ uptake for each tracer was expressed as a percentage of the injected dose. The injected dose was calculated by multiplying the initial plasma counts (2-min time point) by the estimated plasma volume.

2.8. Fecal cholesterol extraction

Fecal cholesterol was extracted as previously described [14], with minor modifications. The total feces collected from 0 to 48 h were weighed and soaked in Millipore water (1 mL water per 100 mg feces) overnight at 4 °C. The following day, an equal volume of absolute ethanol

was added, and the mixtures were homogenized. To extract the ^{3}H-cholesterol fractions, 1 mL of the homogenized samples was combined with 1 mL ethanol, a known amount of ^{14}C-cholic acid as an internal standard, and 200 μL NaOH. The samples were saponified at 95 °C for 1 h and cooled to room temperature, and then ^{3}H-cholesterol was extracted 2× with 3 mL hexane. The extracts were pooled, evaporated, resuspended in toluene, and then counted in a liquid scintillation counter.

2.9. RNA extraction and gene expression analysis

Tissue for mRNA analysis was homogenized, and RNA was isolated using Trizol (Invitrogen, Carlsbad, CA) reagent according to the manufacturer's instructions. Real-time quantitative polymerase chain reaction (PCR) assays were performed with an Applied Biosystems 7300 sequence detector. Briefly, 5 μg of total RNA was reverse transcribed with the use of an Applied Biosystems High Capacity cDNA archive kit (Applied Biosystems, Foster City, CA) according to the manufacturer's instructions. Each 25-μL amplification reaction contained 100 ng cDNA, 900 nmol/L forward primer, 900 nmol/L reverse primer, 200 nmol/L fluorescent probe, and 2× universal PCR master mix. Primer and probe sequences are available on request. Data were expressed as fold change ±SD versus control and normalized to β-actin mRNA.

2.10. Protein analysis by Western blotting

Adipose tissue and liver were homogenized in TES buffer (20 mM Tris, pH7.4, 1 mM EDTA, 250 mM sucrose and 1 mM PMSF). Protein contents were determined by BCA assay and Western blot analysis performed as described previously [17].

2.11. Statistical analysis

Values are presented as mean ± SEM or ± SD as indicated. Comparisons of mean values between groups were evaluated using Student's two-tailed unpaired *t* test, with the use of GraphPad Prism Software. Differences were considered significant at a two-tailed *p*-value of <0.05.

3. Results

3.1. PPARγ agonist GW7845 reduces fecal sterol excretion in vivo

Treatment with GW7845 (20 mg/kg/day) for 2 weeks in mice led to non-significant trends towards decreases in plasma total cholesterol (83.3 ± 8.8 in control group vs. 63.2 ± 9.8 mg/dL GW7845 treated group), HDL-cholesterol (54.3 ± 4.0 in control group vs. 44.3 ± 7.4 mg/dL GW7845 treated group) or triglycerides (43 ± 8.5 in control group vs. 39± 4.7 mg/dL in GW7845 treated group). Body weights of mice were evaluated before and after 2 weeks of treatment, and there was no statistically significant difference in weight gain between the control group versus the GW7845 treated group (1.62 ± 0.37 g in control group vs. 2.06 ± 0.73 g in GW7845 treated group, $P = 0.21$).

To test the hypothesis that PPARγ activation promotes reverse cholesterol transport in vivo, cholesterol-loaded ^{3}H-cholesterol labeled J774 macrophages were injected intra-peritoneally into wild type C57BL6/J mice fed with GW7845 or control diet. As shown in Fig. 1A, ^{3}H-tracer present in plasma was unchanged in GW7845-treated mice over the timecourse examined (at 6, 24 and 48 h). At the same time, we saw a 43% decrease ($P < 0.05$) in the radioactivity recovered after free sterol extraction from the feces (Fig. 1B). These data indicate that PPARγ activation by agonist GW7845 decreased fecal free sterol excretion without any major change in plasma levels of ^{3}H-tracer.

3.2. PPARγ agonist GW7845 has no effect on total free cholesterol efflux in vitro

To investigate whether PPARγ activation influences the ability of HDL to accept cholesterol effluxed from macrophages, we incubated serum collected from mice fed control diet or diet containing PPARγ agonist GW7845 with labeled bone marrow macrophages. The bone marrow macrophages were cholesterol-loaded with acetylated LDL to simulate foam cell formation. Efflux studies were performed in presence/absence of probucol, an inhibitor of ABCA1 activity, to differentiate ABCA1 dependent from ABCA1 independent efflux. There was a significant 46% increase in ABCA1-mediated efflux to serum from PPARγ treated mice ($P < 0.05$) (Fig. 2). There was no change in the non-ABCA1 mediated efflux, with a resultant non-significant trend towards an increase total cholesterol efflux. These data suggest that macrophage cholesterol efflux is not inhibited by PPARγ, and cannot account for the decrease of tracer in feces.

3.3. PPARγ agonist GW7845 has no effect on HDL cholesteryl ester catabolism, but increases uptake of HDL-derived cholesterol by adipose tissue, with a concomitant decrease in uptake by the liver

To further characterize the effects of PPARγ agonist GW7845 on reverse cholesterol transport, human HDL labeled with ^{3}H-cholesteryl ether was injected by tail vein in wild type C57BL6/J mice after 2 weeks of GW7845 treatment (20 mg/kg/day). Cholesteryl ether, unlike cholesteryl ester, is not metabolized and is trapped in lysosomes once taken up by tissues. There was no effect of PPARγ agonism on the ^{3}H-cholesteryl ether-HDL fractional catabolic rate (0.101 ± 0.023 versus 0.089 ± 0.008%/h) indicating ^{3}H-cholesteryl ether plasma clearance was not different between groups (Fig. 3A).

Interestingly, hepatic uptake of ^{3}H-cholesteryl ether was decreased by 22% ($P < 0.05$) (Fig. 3B) and adipose tissue uptake was significantly increased by more than two-fold ($P < 0.005$) with drug treatment (Fig. 3C). These data indicate that PPARγ activation with the agonist GW7845 decreases fecal excretion of HDL derived cholesterol by redirecting cholesterol for uptake by adipose tissue. There was no difference in liver weights (1.35 ± 0.12 in control group vs. 1.36 ± 0.15 g in GW7845 treated group; $P = 0.90$). Inguinal adipose tissue weights appeared to be trending up in the GW7845 treated group, but was not statistically significantly different from control group (0.190 ± 0.015 in control group vs. 0.217 ± 0.028 g in GW7845 treated group; $P = 0.06$). Hence, the effects on the % CPM injected per g excised tissues (Fig. 3B and C) were not due to significantly altered organ weights.

3.4. PPARγ agonist GW7845 increases SR-BI mRNA and protein expression in adipose tissue

We next sought to determine a mechanism by which PPARγ agonist GW7845 may be increasing HDL cholesterol uptake by adipose tissue. The scavenger receptor type-BI (SR-BI) emerged as a plausible candidate. SR-BI is known to be a membrane transporter involved in the selective uptake of cholesteryl esters from HDL [18]. Gene expression of SR-BI was measured in liver and adipose tissue by real time PCR. As shown in Fig. 4A, GW7845 treatment significantly upregulated hepatic mRNA expression of SR-BI (1.5-fold, $P < 0.05$), as well as CD36 (a known PPARγ target gene in the liver), but this did not translate into any significant changes on SR-BI protein expression in the liver (Fig. 4C). In contrast, there was a significant increase in adipose tissue SR-BI mRNA expression (3.5-fold, $P < 0.05$) (Fig. 4B) as well as SR-BI protein expression (Fig. 4D), which could result in increased HDL cholesterol uptake into adipose tissue. FABP4, a known PPARγ target gene in adipose tissue was also significantly upregulated.

3.5. SR-BI is involved in the redirection of cholesterol effluxed from macrophages for uptake by adipose tissue in vivo

To directly determine whether the redirection of effluxed cholesterol from macrophages for adipose tissue uptake involved SR-BI in vivo, we performed HDL turnover and uptake experiments in SR-BI knockout mice treated with the PPARγ agonist GW7845 at 20 mg/kg/day or standard chow diet for 2 weeks. In these mice, GW7845 treatment did not lead to any significant difference in ^{3}H-cholesteryl ether labeled HDL uptake in liver (Fig. 4E) or adipose tissue (Fig. 4F) 48 h after administration of tracer, demonstrating that the effect of PPARγ agonist treatment in increasing HDL-derived cholesterol uptake by adipose tissue involves SR-BI. There was no difference in liver weights (1.48 ± 0.17 in control group vs. 1.40 ± 0.18 g in GW7845 treated group; $P = 0.43$), inguinal adipose tissue depot weights (0.277 ± 0.089 in control group vs. 0.295 ± 0.070 g in GW7845 treated group; $P = 0.71$), or total body weight gain over 2 weeks (1.69 ± 0.31 in control group vs. 2.32 ± 1.04 g in GW7845 treated group; $P = 0.18$).

4. Discussion

The present study shows that activation of PPARγ with a potent and selective PPARγ agonist, GW7845, redirects cholesterol effluxed by macrophages towards uptake by adipose tissue. The effects of GW7845 on glucose homeostasis in mice have previously been described [6]. As expected from the PPARγ agonist class of drugs, GW7845 treatment in mice led to significantly lower fasting insulin levels and improved insulin sensitivity (as measured by insulin response to glucose challenge), and this was thought to correlate with its antiatherogenic effect [6]. Here, we first directly demonstrated that the radioactivity recovered into the fecal free sterol fraction after ^{3}H-cholesterol-labeled macrophage injection was significantly lower in mice treated with the PPARγ agonist GW7845, implying decreased macrophage to feces reverse cholesterol transport in vivo. This decrease was not associated with a major change in ^{3}H-cholesterol counts in plasma or tissues examined (including liver and adipose; Supplemental Fig. 1) in the in vivo macrophage RCT assay. This is not entirely unexpected as RCT is a dynamic process; hence, while counts in the feces reflect net RCT flux, counts in intermediate tissues in the RCT pathway at a particular time-point may not reflect actual total cholesterol flux to that particular tissue. Therefore, we then investigated whether serum from GW7845 treated mice would affect macrophage free cholesterol efflux by using mouse bone marrow macrophages. Since fecal sterol excretion was reduced by PPARγ agonist treatment, we reasoned that this may be due to inhibition of macrophage cholesterol efflux, the first step of the RCT pathway. Contrary to this hypothesis, we saw a significant 46% increase in ABCA1-mediated efflux to serum from PPARγ agonist treated mice, when cells were incubated with acetylated LDL.

Others have showed that macrophages pre-treated with PPARγ agonist GW7845 or rosiglitazone have higher expression of macrophage ABCA1 and ABCG1 [12,13]. In THP1 macrophages, macrophage PPARγ activation has been shown to promote ABCA1-mediated apoA-I specific efflux, as well as ABCG-1 mediated efflux to HDL3 as a cholesterol acceptor. We have conducted similar studies in J774 macrophages and bone marrow macrophages, in which macrophages were pre-treated with the PPARγ agonist GW7845. We found that PPARγ agonist treatment led to no significant change in total cholesterol efflux to 2.5% human serum, but promoted ABCA1-mediated apolipoprotein A-I specific efflux, and ABCG-1 mediated efflux to HDL3 (unpublished), consistent with previously published literature [12,13]. Overall, these data suggest that PPARγ activation does not inhibit macrophage cholesterol efflux, but instead can potentially increase macrophage to serum efflux capacity via both improvement in HDL function as acceptor, as well as upregulation of macrophage ABCA1 and ABCG1 expression.

It is interesting to note that PPARγ activation in human macrophage increases ABCA1 and ABCG1 gene expression but also the expression of other crucial genes involved in the uptake of oxidized LDL, such as CD36 [18]. Increased CD36 expression can lead to intracellular accumulation of cholesterol and production of natural PPARγ ligands. This leads to further activation of PPARγ, potentially creating an unwanted positive feedback cycle of ever increasing lipid accumulation and conversion of macrophages into atherogenic foam cells. However, despite increased oxidized LDL uptake, PPARγ activation has been shown to inhibit foam cell formation through enhanced cholesterol efflux [19]. In the present study, total efflux capacities of serum from GW7845-treated mice were not statistically different from control-treated mice despite the 46% increase in ABCA1-mediated efflux. Overall, these results indicate that PPARγ activation modulates some aspects of macrophage lipid homeostasis (including ABCA1-mediated cholesterol efflux) but may not necessarily be effective in promoting net macrophage cholesterol efflux. Some of these differences may be explained by the fact that the relative contribution of different cholesterol transporters (ABCA1, ABCG1 and SR-BI) to efflux can vary with different macrophage cell models, and under different conditions.

Based on these data, we next investigated the plasma removal of HDL cholesterol using ^{3}H-cholesteryl ether-labeled HDL kinetics. Kinetic parameters show that PPARγ activation has no effect on catabolism of HDL-cholesteryl esters, assessed using ^{3}H-cholesteryl ether-labeled HDL. Interestingly, uptake of ^{3}H-cholesteryl ether-labeled HDL was decreased in liver but increased in adipose tissue. Hence, these data indicate that overall plasma removal of HDL-cholesterol is not modified under PPARγ activation as there is redirection of HDL-cholesterol uptake from liver to adipose tissue.

Activation of PPARγ has previously been shown to increase hepatocyte SR-BI expression, as PPARγ binds to a response element in the human SR-BI promoter [20]. The pivotal role of SR-BI as a membrane transporter involved in the selective uptake of cholesteryl esters from HDL [21] in steroidogenic tissues and the liver has been well established. SR-BI is also abundantly expressed in adipocytes, but little is known about its function and regulation in these cells. Yvan-Charvet et al. [22] reported that SR-BI provides an important source of cholesterol in adipose cell lines, and under certain conditions such as insulin and angiotensin II treatment, there is induction of expression and translocation of this receptor leading to an increase in cholesterol influx and storage in adipose tissue. We reasoned that PPARγ agonists may exert a similar effect and investigated whether PPARγ agonist treatment led to changes in expression of SR-BI in liver and/or adipose tissue. Indeed, we saw an upregulation of adipose tissue SR-BI mRNA and protein in PPARγ agonist treated mice. Even though SR-BI mRNA was also upregulated by PPARγ activation in liver, this did not translate into an upregulation of hepatic SR-BI protein, suggesting that PPARγ activation may also play a role in the post-transcriptional processing of SR-BI.

To confirm that SR-BI plays a role in the increase of HDL-derived cholesterol uptake by adipose tissue in response to PPARγ agonist treatment, we then performed in vivo experiments to examine ^{3}H-cholesteryl ether labeled HDL3 turnover and uptake in SR-BI knockout mice treated with PPARγ agonist GW7845 or control chow diet. In SR-BI knockout mice, PPARγ activation did not have the same effect on HDL metabolism and tissue uptake seen in wild-type mice. Our data reveal that the selective uptake of cholesteryl ester from HDL in adipose tissue via SR-BI is functional in vivo and can be regulated by PPARγ activation.

Our observations highlight currently underappreciated interactions between adipose tissue and HDL cholesterol, and modulation of these interactions by PPARγ activation, such that adipose tissue may play an important role in reverse cholesterol transport. Clinical

observations have found a correlation between PPARγ agonist treatment and increased adiposity, but the overall impact of PPARγ agonist on cardiovascular risk remains controversial [7,8]. Based on our findings, one could speculate that by redirecting cholesterol to adipose and keeping excess cholesterol out of macrophages in the atherosclerotic plaque, PPARγ agonist treatment could have overall beneficial effects on atherosclerosis. On the flipside, these benefits could potentially be outweighed by increased adiposity and obesity. Of note, there was no significant difference in body weight or inguinal adipose tissue weights between control and PPARγ agonist treated groups during the time period examined. It is possible that differences in body weight or adipose tissue mass could become apparent with longer durations of treatment, and a limitation of our study is that this was only examined at 2 weeks. Clinical observations that significant correlations could be described between plasma cholesterol and various indices of obesity [23] and that plasma cholesterol rose and fell as body weight was lost and gained, respectively [24], suggest that adipose tissue likely plays an important role in cholesterol metabolism. Krause and Hartman have proposed that adipose tissue might be able to "buffer" an increase in plasma cholesterol by its ability to take up cholesterol for storage [25], and our data suggest that PPARγ agonists may enhance adipocyte function in this regard and redirect cholesterol effluxed from macrophages to adipose tissue. A limitation of our study is that human lipoprotein metabolism was studied in animal models, and although relevant mouse models were used, one would have to be cautious with wider extrapolations of the data to humans.

Based on our current understanding, it appears that there exists a previously underappreciated model for HDL-adipose interaction – under certain conditions such as refeeding, insulin, angiotensin II treatment; there is increased uptake of HDL cholesterol by adipose tissue via SR-BI [22]. We have demonstrated here that PPARγ agonists can have the same effect. On the other hand, cholesterol efflux from adipose tissue via ABCA1 has been demonstrated under other conditions such as TNF-alpha treatment [26] and prolonged lipolysis [27]. Whether PPARγ agonist treatment has an effect on cholesterol efflux from adipose tissue and if so, to what extent does it influence net flux of cholesterol under different conditions, deserves further study. Such insights may lead to improved understanding of adipose tissue function as it pertains to HDL metabolism, such that therapeutic optimization for the use of PPARγ agonists in insulin resistance, dyslipidemia, obesity and atherosclerosis can be better achieved.

Abbreviations

HDL-C	high density lipoprotein cholesterol
CVD	cardiovascular disease
RCT	reverse cholesterol transport
ABCA1	ATP binding cassette transporter A1
ABCG1	ATP binding cassette transporter G1
SR-BI	scavenger receptor type-BI

Acknowledgments

We are indebted to Dawn Marchadier, Hui Li, Aisha Wilson, Edwige Edouard, David Chang, Michelle Joshi, Christine Hinkle, Fiona McGillicuddy and Debra Cromley of the University of Pennsylvania, for their excellent technical assistance. We also thank GlaxoSmithKline for providing GW7845. This work was supported by P01-HL22633 and P01-HL59407 from the National Heart, Lung, and Blood Institute, and an Alternative Drug Discovery Initiative award to the University of Pennsylvania from GlaxoSmithKline. S.T. was supported by a fellowship of the American Heart Association (0315294T) and the Institute for Translational Medicine and

Therapeutics, University of Pennsylvania School of Medicine. Parts of this manuscript were presented in abstract form at the 2008 American Heart Association 57th Annual Scientific Session, New Orleans, LA, November 8–12, 2008.

References

1. Barak Y, Nelson MC, Ong ES, Jones YZ, Ruiz-Lozano P, Chien KR, et al. PPAR gamma is required for placental, cardiac, and adipose tissue development. Mol Cell. 1999 October 4.4:585–595. [PubMed: 10549290]
2. Rosen ED, Sarraf P, Troy AE, Bradwin G, Moore K, Milstone DS, et al. PPAR gamma is required for the differentiation of adipose tissue in vivo and in vitro. Mol Cell. 1999 October 4.4:611–617. [PubMed: 10549292]
3. Nagy L, Tontonoz P, Alvarez JG, Chen H, Evans RM. Oxidized LDLregulates macrophage gene expression through ligand activation of PPARgamma. Cell. 1998 April 2.93:229–240. [PubMed: 9568715]
4. Lehmann JM, Moore LB, Smith-Oliver TA, Wilkison WO, Willson TM, Kliewer SA. An antidiabetic thiazolidinedione is a high affinity ligand for peroxisome proliferator-activated receptor gamma (PPAR gamma). J Biol Chem. 1995 June 22.270:12953–12956. [PubMed: 7768881]
5. Yki-Järvinen H. Thiazolidinediones. N Engl J Med. 2004 September 11.351:1106–1118. [PubMed: 15356308]
6. Li AC, Brown KK, Silvestre MJ, Willson TM, Palinski W, Glass CK. Peroxisome proliferator-activated receptor gamma ligands inhibit development of atherosclerosis in LDL receptor-deficient mice. J Clin Invest. 2000 August 4.106:523–531. [PubMed: 10953027]
7. Nissen SE, Wolski K. Effect of rosiglitazone on the risk of myocardial infarction and death from cardiovascular causes. N Engl J Med. 2007 June 24.356:2457–2471. [PubMed: 17517853]
8. Lipscombe LL, Gomes T, Lévesque LE, Hux JE, Juurlink DN, Alter DA. Thiazolidinediones and cardiovascular outcomes in older patients with diabetes. JAMA. 2007 December 22.298:2634–2643. [PubMed: 18073359]
9. Lewis GF, Rader DJ. New insights into the regulation of HDL metabolism and reverse cholesterol transport. Circ Res. 2005 June 12.96:1221–1232. [PubMed: 15976321]
10. Tanigawa H, Billheimer JT, Tohyama J, Zhang Y, Rothblat G, Rader DJ. Expression of cholesteryl ester transfer protein in mice promotes macrophage reverse cholesterol transport. Circulation. 2007 September 11.116:1267–1273. [PubMed: 17709636]
11. Goldberg RB, Kendall JT, Deeg DM, Buse MA, Zagar JB, Pinaire AJ. GLAI Study Investigators. A comparison of lipid and glycemic effects of pioglitazone and rosiglitazone in patients with type 2 diabetes and dyslipidemia. Diabetes Care. 2005 July 7.28:1547–1554. [PubMed: 15983299]
12. Chawla A, Boisvert WA, Lee CH, Laffitte BA, Barak Y, Joseph SB, et al. PPAR gamma-LXR-ABCA1 pathway in macrophages is involved in cholesterol efflux and atherogenesis. Mol Cell. 2001 January 1.7:161–171. [PubMed: 11172721]
13. Chinetti G, Lestavel S, Bocher V, Remaley AT, Neve B, Torra IP, et al. PPAR-alpha and PPAR-gamma activators induce cholesterol removal from human macrophage foam cells through stimulation of the ABCA1 pathway. Nat Med. 2001 January 1.7:53–58. [PubMed: 11135616]
14. Naik SU, Wang X, Da Silva JS, Jaye M, Macphee CH, Reilly MP, et al. Pharmacological activation of liver X receptors promotes reverse cholesterol transport in vivo. Circulation. 2006; 113:90–97. [PubMed: 16365197]
15. Tietge UJ, Maugeais C, Cain W, Grass D, Glick JM, de Beer FC, et al. Overexpression of secretory phospholipase A(2) causes rapid catabolism and altered tissue uptake of high density lipoprotein cholesteryl ester and apolipoprotein A-I. J Biol Chem. 2000; 275:10077–10084. [PubMed: 10744687]
16. Bligh EG, Dyer WJ. A rapid method of total lipid extraction and purification. Can J Biochem Physiol. 1959; 37:911–917. [PubMed: 13671378]
17. Dagher G, Donne N, Klein C, Ferre P, Dugail I. HDL-mediated cholesterol uptake and targeting to lipid droplets in adipocytes. J Lipid Res. 2003; 44:1811–1820. [PubMed: 12867544]

18. Nagy L, Tontonoz P, Alvarez JG, Chen H, Evans RM. Oxidized LDL regulates macrophage gene expression through ligand activation of PPARgamma. Cell. 1998 April 2.93:229–240. [PubMed: 9568715]

19. Argmann CA, Sawyez CG, McNeil CJ, Hegele RA, Huff HW. Activation of peroxisome proliferator-activated receptor gamma and retinoid X receptor results in net depletion of cellular cholesteryl esters in macrophages exposed to oxidized lipoproteins. Arterioscler Thromb Vasc Biol. 2003 March 3.23:475–482. [PubMed: 12615696]

20. Malerød L, Sporstøl M, Juvet LK, Mousavi A, Gjøen T, Berg T. Hepatic scavenger receptor class B, type I is stimulated by peroxisome proliferator-activated receptor gamma and hepatocyte nuclear factor 4alpha. Biochem Biophys Res Commun. 2003 June 3.305:557–565. [PubMed: 12763030]

21. Acton S, Rigotti A, Landschulz KT, Xu S, Hobbs HH, Krieger Ml. Identification of scavenger receptor SR-BI as a high density lipoprotein receptor. Science. 1996; 271:518–520. [PubMed: 8560269]

22. Yvan-Charvet L, Bobard A, Bossard P, Massiéra F, Rousset X, Ailhaud G, et al. In vivo evidence for a role of adipose tissue SR-BI in the nutrional and hormonal regulation by adiposity and cholesterol homeosyasis. Areterioscler Throm Vasc Biol. 2007; 27:1340–1345.

23. Montoye HJ, Epstein FH, Kjelsberg MO. Relationship between serum cholesterol and body fatness. An epidemiologic study. Am J Clin Nutr. 1966 June 6.18:397–406. [PubMed: 5938192]

24. Galbraith WB, Connor WE, Stone DB. Weight loss and serum lipid changes in obese subjects given low calorie diets of varied cholesterol content. Ann Intern Med. 1966 February 2.64:268–275. [PubMed: 5902274]

25. Krause BR, Hartman AD. Adipose tissue and cholesterol metabolism. J Lipid Res. 1984; 25:97–110. [PubMed: 6368715]

26. Zhao SP, Dong SZ. Effect of tumor necrosis factor alpha on cholesterol efflux in adipocytes. Clin Chim Acta. 2008 March 1–2.389:67–71. [PubMed: 18155667]

27. Verghese PB, Arrese EL, Soulages JL. Stimulation of lipolysis enhances the rate of cholesterol efflux to HDL in adipocytes. Mol Cell Biochem. 2007 August 1–2.302:241–248. [PubMed: 17390217]

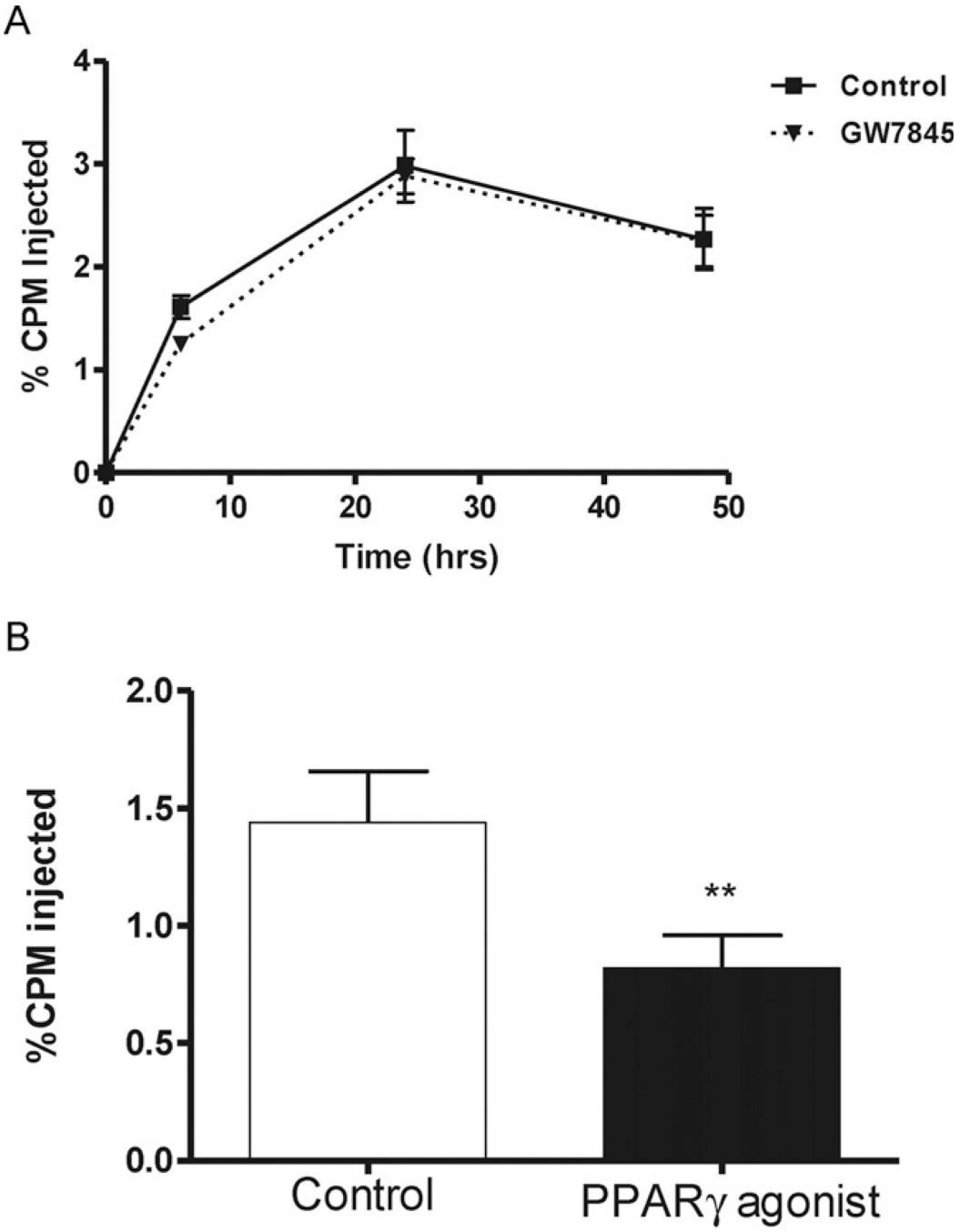

Fig. 1.

(A) Time course of plasma ^{3}H-cholesterol distribution over 48 h in control (solid line) and GW7845 treated (dotted line) C57BL6/J mice. C57BL/6 mice were fed with either control chow diet or PPARγ agonist GW7845 supplemented chow diet for two weeks before ^{3}H-cholesterol-labeled J774 cells were injected intraperitoneally (4.5×10^{6} cells containing 4×10^{6} cpm in 0.5 mL medium). Mice were bled at 6, 24, and 48 h after injection. Data are expressed as percent cpm injected ± SEM. Data represent combined results from 4 independent experiments, $n = 6$ mice per group per experiment. (**$P < 0.05$ vs. control group). (B) Fecal ^{3}H-free sterol tracer excretion 48 h after injection of ^{3}H-cholesterol-labeled macrophages in control (white bar) and GW7845 treated (black bar) C57BL6/J mice.

C57BL/6 mice were fed with either control chow diet or PPARγ agonist GW7845 supplemented chow diet for two weeks before ^{3}H-cholesterol-labeled J774 cells were injected, and feces were collected continuously from 0 to 48 h. Data are expressed as percent cpm injected ± SEM. Data represent combined results from 4 independent experiments, n = 6 mice per group per experiment. (**$P < 0.05$ vs. control group).

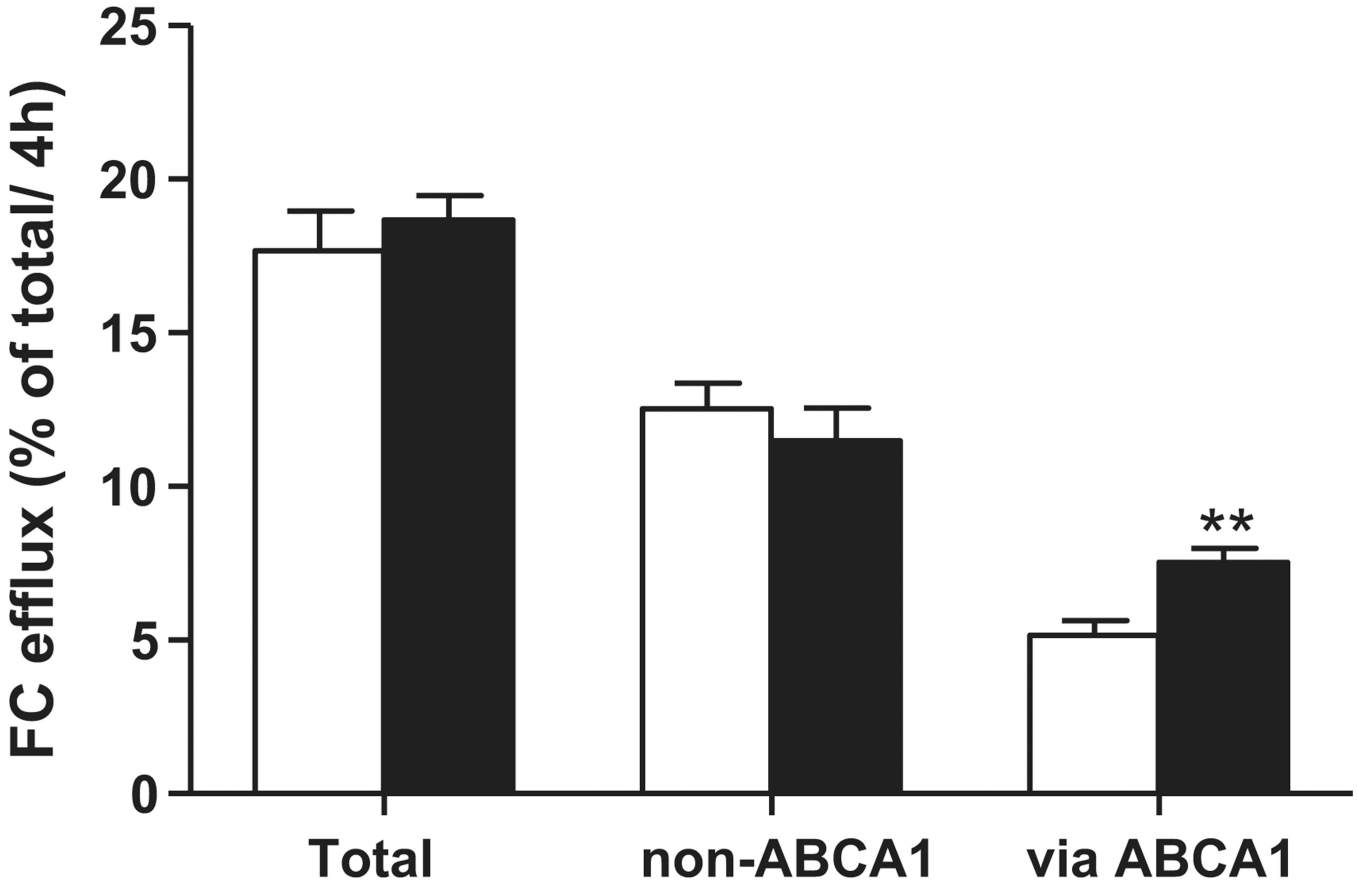

Fig. 2.

Free cholesterol efflux from C57BL6/J bone marrow macrophages loaded with acetylated LDL was determined in the presence of serum from control mouse (white bars) or GW7845 treated mouse (black bars). Probucol (20 μM) was added to obtain non-ABCA1 mediated efflux and ABCA1 mediated efflux was obtained by subtraction. Efflux of free cholesterol into the media is expressed as percentage of the total radioactivity in the media and cells (^{3}H-cholesterol in the medium × 100)/(^{3}H-cholesterol in medium + ^{3}H-cholesterol in the cells). Values represent the average of triplicate determinations (mean ± SD) (**$P < 0.05$).

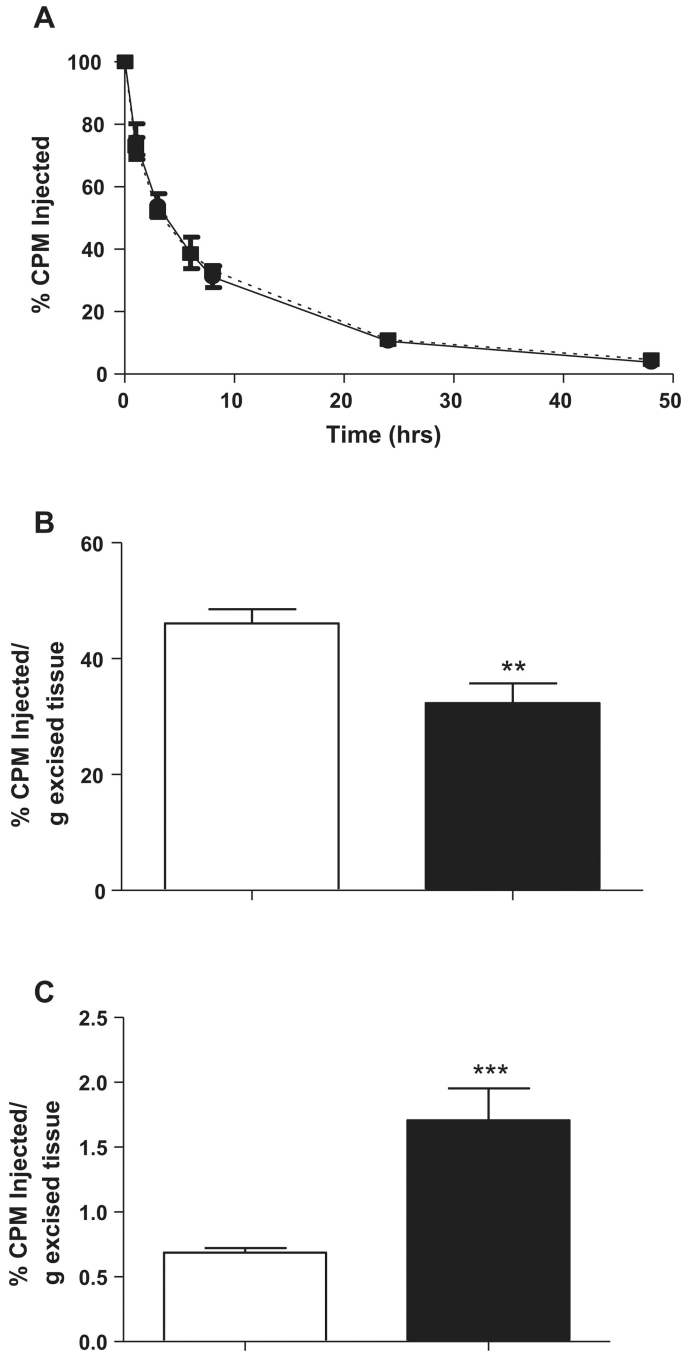

Fig. 3.

(A) Plasma decay curve of ^{3}H-cholesteryl ether in C57BL/6 mice fed a control chow diet (solid line) or GW7845 diet (20 mg/kg/day) for 2 weeks (dotted line). (B) Uptake of ^{3}H-cholesteryl ether labeled HDL in liver 48 h after administration of tracer in control (white bar) and GW7845 treated (black bar) C57BL6/J mice. Data are expressed as percent cpm injected ± SEM, n = 6 mice per group (**P < 0.05 vs. control group). (C) Uptake of [^{3}H]-cholesteryl ether labeled HDL in inguinal adipose tissue 48 h after administration of tracer in control (white bar) and GW7845 treated (black bar) C57BL6/J mice. Data are expressed as percent cpm injected ± SEM, n = 6 mice per group. (***P < 0.005 vs. control group).

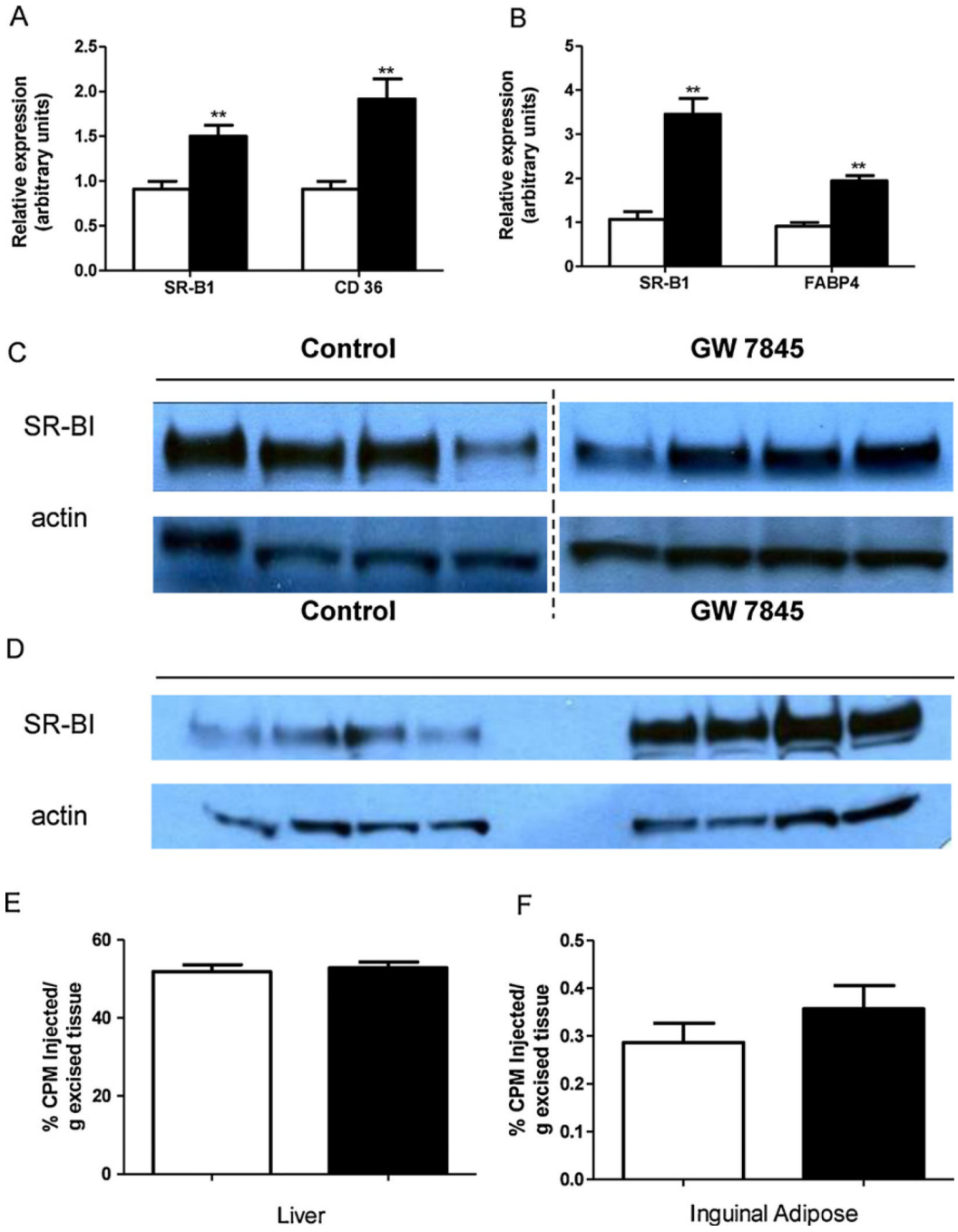

Fig. 4.

Animals were fed either control chow diet or PPARγ agonist GW7845 supplemented chow diet for two weeks. (A) Liver gene expression analysis in wild-type mice determined by real-time PCR analysis. mRNA expression of SR-BI and CD36 in liver of control (white bars) and GW7845 treated (black bars) C57BL6/J mice. Data are expressed as fold change ± SEM vs. control group mice and normalized to beta-actin mRNA. Results are representative of 2 independent experiments, *n* = 6 mice per group per experiment. (B) Adipose tissue gene expression analysis in wild-type mice determined by real-time PCR analysis. mRNA expression of SR-BI and FABP4 in inguinal adipose tissue from control (white bars) and GW7845 treated (black bars) C57BL6/J mice. Data are expressed as fold change ± SEM vs.

control group mice and normalized to beta-actin mRNA. Results are representative of 2 independent experiments, n = 6 mice per group per experiment. (C) Protein expression by Western blot analysis of SR-BI in liver tissue from control and GW7845 treated C57BL6/J mice. The Western blots for SR-BI and actin from livers of both control and GW7845 treated mice represent groupings of images from different parts of the same gel, with the same exposure. (D) Protein expression by Western blot analysis of SR-BI in inguinal adipose tissue from control and GW7845 treated C57BL6/J mice. (E) Uptake of ^{3}H-cholesteryl ether labeled HDL in liver 48 h after administration of tracer in control (white bar) and GW7845 treated (black bar) SR-BI knockout mice, n = 6 mice per group. (F) Uptake of ^{3}H-cholesteryl ether labeled HDL in inguinal adipose tissue 48 h after administration of tracer in control (white bar) and GW7845 treated (black bar) SR-BI knockout mice. n = 6 mice per group.